A framework for predicting accuracy limitations in large-eddy simulation

Bernard J. Geurts [‡]
Faculty of Mathematical Sciences, J.M. Burgers Center, University of Twente
P.O. Box 217, 7500 AE Enschede, The Netherlands

Jochen Fröhlich
Institute for Hydromechanics, University of Karlsruhe, Kaiserstrasse 12
76128 Karlsruhe, Germany

The accuracy of large-eddy simulations is limited, among others, by the quality of the subgrid parameterization and the numerical contamination of the smaller retained flow-structures. We characterize the total simulation-error in terms of the 'subgrid-activity' s, which measures the relative turbulent dissipation-rate ($0 \leq s \leq 1$) and the 'subgrid-resolution' r. This analysis is applied to turbulent mixing of a 'Smagorinsky-fluid' using a finite volume discretization of fourth order accuracy. On fixed coarse grids, i.e., at constant computational cost, the total simulation-error decreases monotonically with filter-width Δ for large s while for smaller s the total error may even increase with decreasing Δ. The corresponding modeling – and spatial discretization-error contributions are quantified at various resolutions.

[‡]Also: Department of Engineering, Queen Mary College, University of London, Mile End, London E1 4NS, United Kingdom

Corresponding author: Bernard J. Geurts
e-mail: b.j.geurts@math.utwente.nl
tel: +32-53-489-4125
fax: +31-53-4894833
PACS numbers: 02.60.Cb, 47.27.Eq

The intricacies of turbulent flow have motivated a number of modeling strategies. These are aimed at reducing the complexity of the underlying dynamical system while reliably predicting the primary flow phenomena. In large-eddy simulation (LES) these conflicting requirements are expressed by coarsening the description on the one hand and capturing the generic flow-features on the other hand. This is achieved by spatial filtering and subgrid modeling. The filter-width, identified with the length-scale parameter Δ in the subgrid model, determines the physical detail retained in the LES solution. How much of this information is actually properly represented numerically is a crucial matter [1], [2], [3].

We quantify the role of the numerical method and the subgrid parameterization in relation to the accuracy achieved. Next to Δ, the main quantity that determines the quality of the solution is the 'subgrid-resolution' $r = h/\Delta$ in which h denotes the mesh-spacing. If $r \ll 1$ then numerical effects are comparably small and a grid-independent solution to the modeled LES equations is approached in which the remaining errors are due to modeling deficiencies. The associated computational cost is, however, comparably large. Conversely, if $r \approx 1$ then physical detail up to scales of order Δ could be retained at smaller computational cost, although numerical effects may substantially contaminate the solution. The difficulty hence resides in assessing the errors and specifying simulation parameters optimal for computational cost.

We simulate the compressible three-dimensional temporal mixing layer in a cubic domain of side-length L. This flow displays a mixing transition to small scales and is characterized by helical pairing. Visualization of the DNS data, obtained on a uniform grid with 192^3 cells, demonstrates the roll-up of the fundamental instability and successive pairings; Fig. 1 displays a well developed state. **2.2: A fourth order accurate, conservative centered finite volume method was adopted for the discretization of the convective terms, in combination with explicit compact storage second order Runge-Kutta time stepping. The time-step was determined according to stability requirements consistent with a fixed CFL number such that temporal integration errors are negligible.** Further details may be found in [4]. The large-eddy simulations were started from a filtered DNS field. First, the DNS field was filtered using a top-hat filter with a width equal to the parameter Δ in the subsequent LES. Second, the data were restricted to the grid employed in the LES. Resolutions 32^3, 48^3, 64^3 and 96^3 and a variety of subgrid resolutions r are included.

We consider LES using Smagorinsky's subgrid model. The turbulent stress tensor τ is modeled according to $\tau_{ij} = -(C_S\Delta)^2|\overline{S}|\overline{S}_{ij}$ where $\overline{S}_{ij} = (\partial\overline{u}_i/\partial x_j + \partial\overline{u}_j/\partial x_i)/2$ is the rate-of-strain tensor, $|\overline{S}|^2 = 2\overline{S}_{ij}\overline{S}_{ij}$ and $C_S = 0.1$ which roughly corresponds to the averaged dynamic coefficient in the developed stages of this flow. The simulation is initiated from the filtered DNS field at $t = 40$, i.e. we skip the transitional regime in which the excessive dissipation of the Smagorinsky model is known to prevent a turbulent flow from developing.

Simulations are performed at different Δ and r. In Fig. 2, the streamwise kinetic energy spectrum $A(k)$ is displayed while the model parameter Δ is reduced together with h such that $r = const.$ On coarser meshes, both large and small scales are changed considerably by changes in resolution. **2.1: The spectrum at low wavenumbers is slightly too low on 32^3 grid points. The numerical contamination and the well-known excessive dissipation of Smagorinsky's model accumulate and show up also in an underprediction of the lower wavenumbers.** At higher resolution a convergence toward the unfiltered DNS spectrum is observed. We also considered simulations in which Δ was kept constant while increasing the resolution, i.e., investigating the limit $r \to 0$ [5]. In this case the grid-independent solution for the Smagorinsky fluid is approached for the corresponding Δ and only errors due to subgrid model deficiencies remain.

In order to quantify the numerical and modeling errors in a concise manner we monitor the volume-averaged resolved kinetic energy,

$$E = \frac{1}{|\Omega|}\int_\Omega \frac{1}{2}\overline{\mathbf{u}}\cdot\overline{\mathbf{u}}\, d\mathbf{x} = \frac{1}{2}\langle\overline{\mathbf{u}}\cdot\overline{\mathbf{u}}\rangle \tag{1}$$

where $\overline{\mathbf{u}}$ is the filtered velocity and $\langle\cdot\rangle$ the average over the flow domain Ω of volume $|\Omega|$. In the developed flow regime E decreases almost linearly with time t [4]. The relative total simulation-error of the quantity E is denoted by δ_E with

$$\delta_E(\Delta, r) = \left\| \frac{(E_{LES}(\Delta, r) - E_{\overline{DNS}}(\Delta, r))}{E_{\overline{DNS}}(\Delta, r)} \right\| \tag{2}$$

where the norm $\|f\|^2 = \int_{t_0}^{t_1} f^2(t)dt/(t_1 - t_0)$ represents time averaging with $t_0 = 40$, $t_1 = 100$. The LES prediction is expressed as E_{LES} and the associated $E_{\overline{DNS}}$ was obtained by top-hat filtering the DNS-data at width Δ and evaluation on the grid with LES-spacing $h = r\Delta$. Here, the notation emphasizes the dependence on Δ and r. A complete simulation is hence characterized by a single number δ_E, which facilitates further comparisons.

For incompressible flow the evolution of E is governed by $\partial E/\partial t = -\langle\varepsilon_t\rangle - \langle\varepsilon_\mu\rangle$, where the turbulent $-$ and molecular dissipation are $\varepsilon_t = -\tau_{ij}\partial_j\overline{u}_i$ and $\varepsilon_\mu = \overline{S}_{ij}\partial_j\overline{u}_i/Re$ with Re the Reynolds number. The amount of turbulent dissipation

is the central quantity used to assess the importance of the subgrid model, i.e., to quantify the amount of modeling in an LES compared to a DNS. We therefore define the subgrid-activity parameter

$$s = \frac{\langle \varepsilon_t \rangle}{\langle \varepsilon_t \rangle + \langle \varepsilon_\mu \rangle} \tag{3}$$

so that by definition $0 \leq s < 1$ with $s = 0$ corresponding to DNS and $s = 1$ to LES at infinite Reynolds number. **1.1: At fixed resolution an increase in the filterwidth Δ implies a decrease of r and an increase in s.**

Given a solution u_i and a filter such that $\overline{u}_i = G * u_i$, an *a priori* link between s and the filter width Δ can be obtained, i.e. a relation $s = s(\Delta)$. If a subgrid model is introduced the same value for s results, provided the model captures the dissipation correctly. **2.3: The relevant subgrid-activity is the value of s which is obtained in an actual LES. This includes a specific subgrid model, e.g. the Smagorinsky model in the present study. For every subgrid model this is uniquely defined and can be obtained during the simulation without further assumptions.** As an illustration we consider the case of isotropic turbulence with three-dimensional energy spectrum $\mathcal{E}(k)$. For the Smagorinsky model we have

$$\langle \varepsilon_t \rangle = (C_S \Delta)^2 \langle |\overline{S}|^3 \rangle \approx C_S^2 \Delta^2 \left(2 \int_0^\infty k^2 (\widehat{G}(k))^2 \mathcal{E}(k) dk \right)^{3/2}$$

with $\widehat{G}$ the Fourier transform of G and $\langle |\overline{S}|^3 \rangle \approx \langle |\overline{S}|^2 \rangle^{3/2}$. Correspondingly, $\langle \varepsilon_t \rangle$ depends on C_S, Δ and parameters specifying $\mathcal{E}$, in particular the Kolmogorov length η. Inserting, e.g., Pao spectrum and Pao filter it reads [6]

$$s = C_S^2 \left((\eta/\Delta)^{4/3} + (1/7)^{4/3} \right)^{-3/2} \tag{4}$$

As $\eta \to 0$ this expression should imply $s \to 1$ which yields $C_s = 1/7$ for the Pao filter (different from the classical value of 0.18 since a filter other than the cut–off filter is used here). The case $\langle \varepsilon_t \rangle = \langle \varepsilon_\mu \rangle$, i.e., $s = 1/2$ further clarifies the interpretation and can be used to distinguish LES from operating either in the inertial or in the dissipation range. According to (4) this corresponds to $\Delta \approx 10.43\eta$. Although Fig. 2 shows that in the present case the spectrum is steeper than $k^{-5/3}$ and the average is also taken in time it turns out that (4) describes the relation $s(\Delta)$ quantitatively correctly if η is properly selected. **1.3: From a curve-fit of (4) to the relation between s and Δ as obtained from the simulations, an extremely good fit of the present data is found when selecting $\eta = 0.0035L$.**

The quantity s constitutes a versatile measure to classify and compare LES solutions since for any subgrid model s can be computed during the simulation. No further assumption on the spectrum and/or on the particular filter is needed. The simulations reported here exhibited time-independency of s with variations < 1 %. **1.1, 2.3: Moreover, variation of r by varying the resolution at fixed Δ displays only a very weak effect on s. The parameters r and s can be regarded as independent and s is primarily a function of Δ.**

Fig. 3 shows the total error δ_E as a function of s. The two regimes for s smaller or larger than 1/2 can be distinguished, indicated by the different slope of the dashed line approximating the data for the highest resolution. **1.2: The error-estimates δ_E for $s \gtrsim 1/2$ at different resolutions almost coincide as a function of s as long as the resolution is adequate, i.e. $r \lesssim 1/2$. In these cases the modeling error dominates. The condition $r \leq 1/2$ corresponds to $s \geq 0.4$ on 64^3; $s \geq 0.51$ on 48^3; $s \geq 0.65$ on 32^3 in the present flow. 1.1: This near collapse of the data as $s \gtrsim 1/2$ strongly favors the use of r and s to characterize the errors over Δ and h separately, from which one could also have started when characterizing the error-dynamics.** For the computationally appealing coarser grids, changing from $r = 1/2$ to $r = 1$ can even result in an increase of the error δ_E, as experienced for 48^3.

We further establish the error-behavior by a decomposition of the error into modeling error and discretization error. LES at a fixed Δ and $r \ll 1$ approaches the grid-independent solution for the Smagorinsky fluid. This solution differs from filtered DNS only because of deficiencies in the subgrid model, which are hence independently quantified by $\delta_{E,m} = \delta_E(\Delta, r \approx 0)$. Likewise, at fixed Δ, comparing LES at a given r with LES at $r \ll 1$ allows to isolate the spatial discretization error $\delta_{E,d}$. It is obtained when in (2) $E_{\overline{DNS}}$ is replaced by $E_{LES}(\Delta, r \approx 0)$. These results are compiled in Fig. 4. **2.4: The results have been grouped according to the resolution and consequently the value of r varies along the curves that represent the discretization error effects.** The magnitude of the numerical error increases with increasing value of r (e.g. for 32^3: $1/4 \leq r \leq 1$; 64^3: $1/8 \leq r \leq 1/2$) and dominates for $r = 1$.

We characterized simulation errors arising in LES of a turbulent mixing layer in terms of the subgrid-activity s and the subgrid-resolution r. Using a time-averaged error norm the behavior of the relevant modeling and discretization errors can be efficiently quantified in this framework.

It is of interest to investigate the error behavior at different flow conditions, e.g., at higher Reynolds numbers, for different numerical methods, e.g., also for second order finite volume and spectral methods, for different flows, e.g., wall-bounded flows, and with different subgrid models. Qualitatively, several limitations for LES corresponding to these extensions can be understood in terms of variations in r and s.

The 'subgrid-activity' s appears to be well-suited for the assessment of different kinds of errors and can be interpreted as a computable replacement for Δ/η. It is even tempting to determine a precise estimate for η by adjusting its value in (4) to match the data of s obtained from actual LES with different values of Δ. This might also be done locally in a statistically stationary inhomogeneous flow, thus extending the present framework to more complex flows. Before being reliable, however, this requires further experience with other configurations. These issues are a subject of ongoing research.

ACKNOWLEDGMENT

JF likes to acknowledge support from the Twente Institute of Mechanics which facilitated his research-visit to the Faculty of Mathematical Sciences in Twente.

---

[1] A.W. Vreman, B.J. Geurts, J.G.M. Kuerten, "Comparison of numerical schemes in Large Eddy Simulation of the temporal mixing layer," *Int.J.Num. Meth. in Fluids* **22**, 299, (1996).

[2] S. Ghosal, "An analysis of numerical errors in large-eddy simulations of turbulence," *J. Comp. Phys.* **125**, 187, (1996).

[3] A.G. Kravchenko and P. Moin "On the effect of numerical errors in large eddy simulation of turbulent flows," *J. Comp. Phys.* **131**, 310, (1997).

[4] A.W. Vreman, B.J. Geurts, J.G.M. Kuerten, "Large-eddy simulation of the turbulent mixing layer," *J. Fluid Mech.* **339**, 357, (1997).

[5] B.J. Geurts, J. Fröhlich, "Numerical effects contaminating LES; a mixed story," *Modern Simulation Strategies for Turbulent Flow*, Edwards. Ed: B.J. Geurts, 317,(2001).

[6] S.B. Pope, *Turbulent Flows*, Cambridge University Press,(2000).

FIG. 1. Snapshot of normal velocity at $t = 80$. The light (dark) iso-surface corresponds to upward (downward) motion.

FIG. 2. Spectra of resolved kinetic energy versus wavenumber at $t = 100$ with different resolutions: 32^3 (solid), 48^3(dashed), 64^3 (dash-dotted) and 96^3 (dotted) keeping $r = 1/2$. Markers correspond to the DNS.

FIG. 3. Relation between relative total error in kinetic energy δ_E and subgrid-activity s. Markers correspond to different resolution: (*): 32^3, (+): 48^3, ($\Box$): 64^3, ($\circ$): 96^3. The dashed line identifies the two regimes discussed in the text.

FIG. 4. Modeling-error $\delta_{E,m}$ (solid, $\circ$) and discretization-error $\delta_{E,d}$ versus subgrid-activity s. Markers correspond to different resolution: (*): 32^3, (+): 48^3, ($\Box$): 64^3.

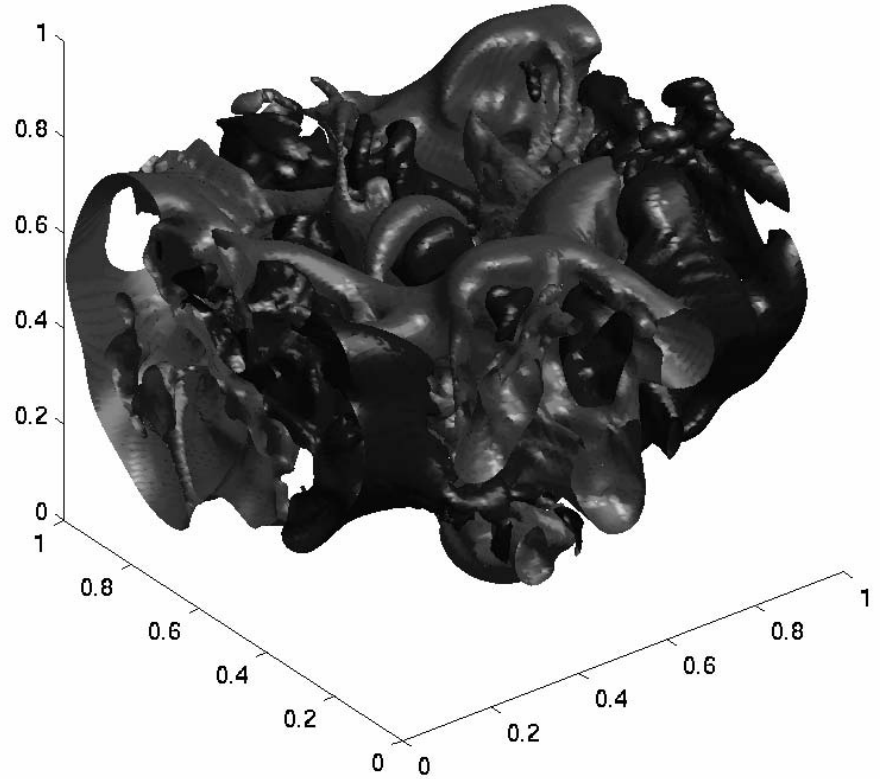

FIG. 1. Snapshot of normal velocity at $t = 80$. The light (dark) iso-surface corresponds to upward (downward) motion.

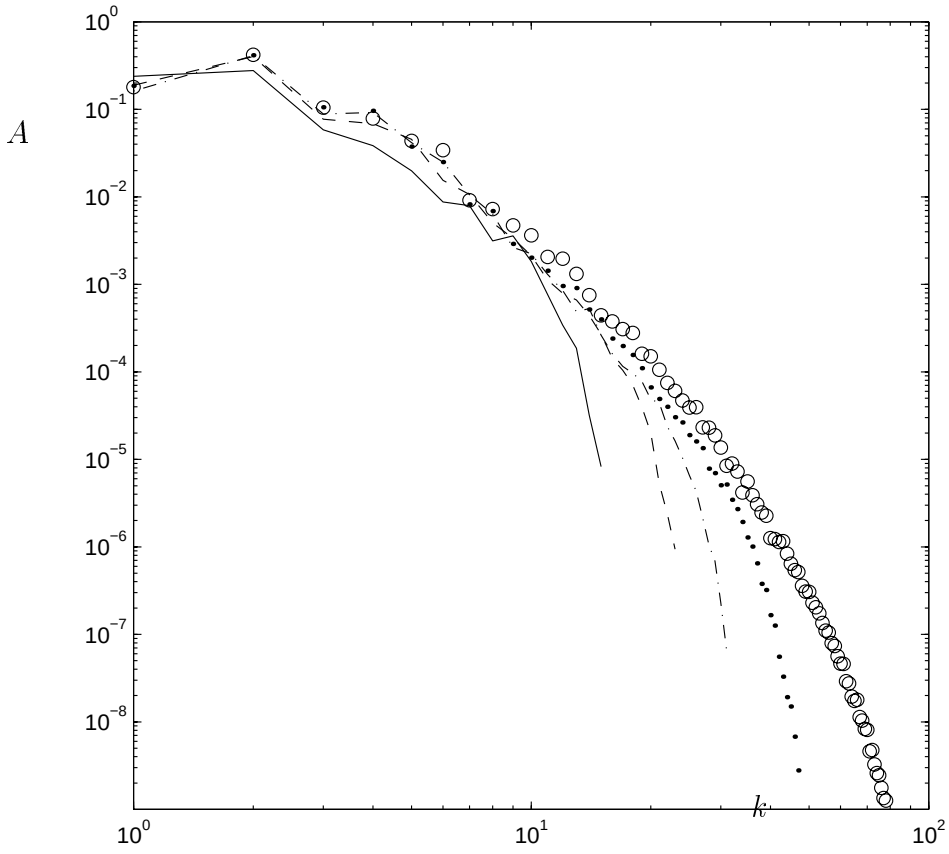

FIG. 2. Spectra of resolved kinetic energy versus wavenumber at $t = 100$ with different resolutions: 32^3 (solid), 48^3(dashed), 64^3 (dash-dotted) and 96^3 (dotted) keeping $r = 1/2$. Markers correspond to the DNS.

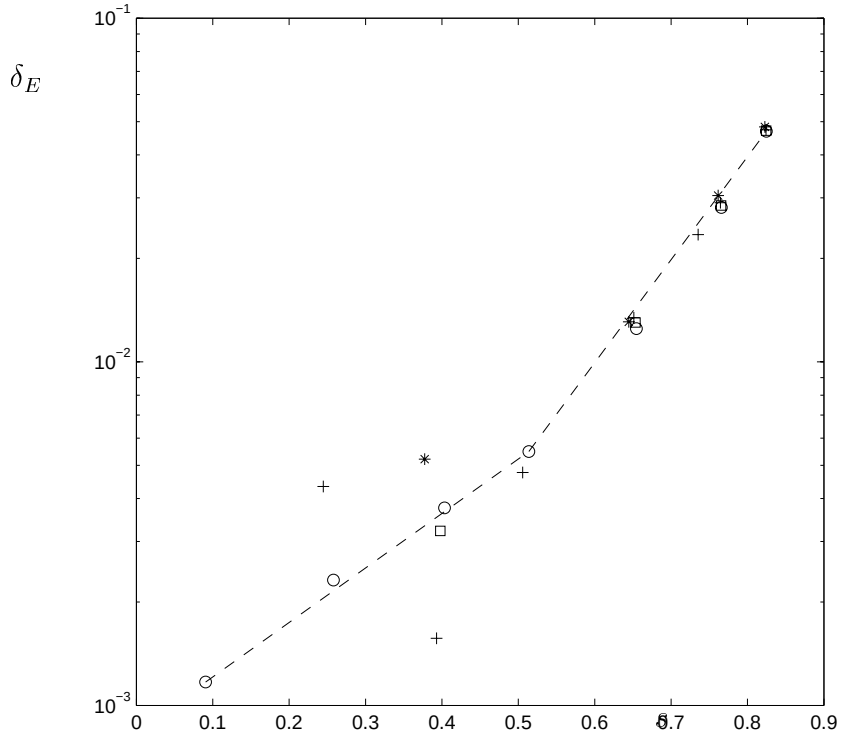

FIG. 3. Relation between relative total error in kinetic energy δ_E and subgrid-activity s. Markers correspond to different resolution: (*): 32^3, (+): 48^3, (□): 64^3, (○): 96^3. The dashed line identifies the two regimes discussed in the text.

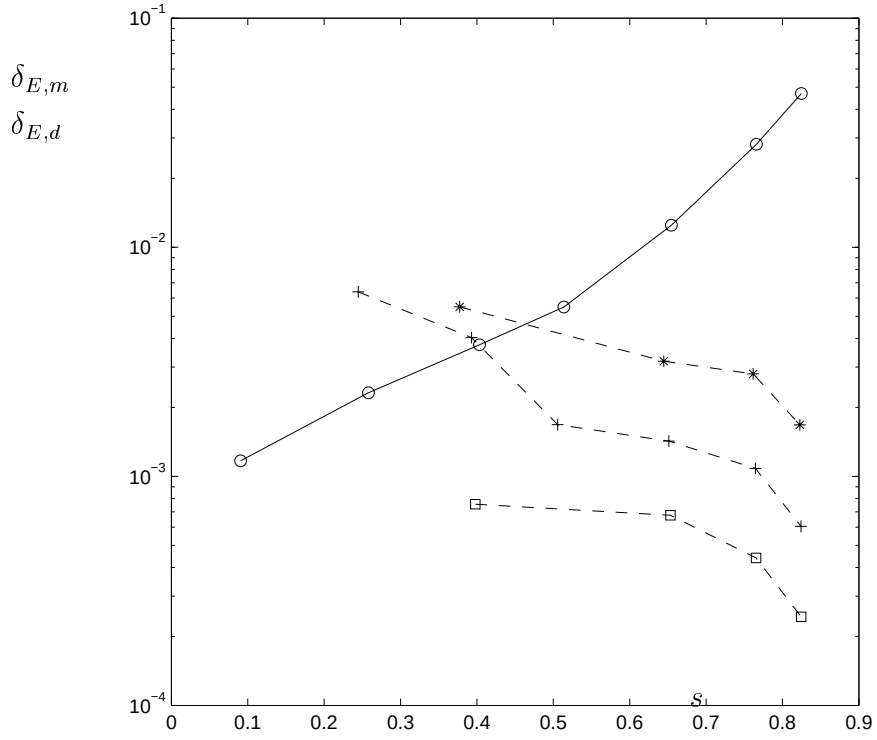

FIG. 4. Modeling-error $\delta_{E,m}$ (solid, $\circ$) and discretization-error $\delta_{E,d}$ versus subgrid-activity s. Markers correspond to different resolution: (*): 32^3, (+): 48^3, ($\Box$): 64^3.